

Search for Supersymmetry in Di-Photon Final States at $\sqrt{s} = 1.96$ TeV

V.M. Abazov³⁶, B. Abbott⁷⁶, M. Abolins⁶⁶, B.S. Acharya²⁹, M. Adams⁵², T. Adams⁵⁰, E. Aguilo⁶, S.H. Ahn³¹, M. Ahsan⁶⁰, G.D. Alexeev³⁶, G. Alkhazov⁴⁰, A. Alton^{65,a}, G. Alverson⁶⁴, G.A. Alves², M. Anastasoie³⁵, L.S. Ancu³⁵, T. Andeen⁵⁴, S. Anderson⁴⁶, B. Andrieu¹⁷, M.S. Anzels⁵⁴, Y. Arnaud¹⁴, M. Arov⁶¹, M. Arthaud¹⁸, A. Askew⁵⁰, B. Åsman⁴¹, A.C.S. Assis Jesus³, O. Atramentov⁵⁰, C. Autermann²¹, C. Avila⁸, C. Ay²⁴, F. Badaud¹³, A. Baden⁶², L. Bagby⁵³, B. Baldin⁵¹, D.V. Bandurin⁶⁰, S. Banerjee²⁹, P. Banerjee²⁹, E. Barberis⁶⁴, A.-F. Barfuss¹⁵, P. Bargassa⁸¹, P. Baringer⁵⁹, J. Barreto², J.F. Bartlett⁵¹, U. Bassler¹⁸, D. Bauer⁴⁴, S. Beale⁶, A. Bean⁵⁹, M. Begalli³, M. Begel⁷², C. Belanger-Champagne⁴¹, L. Bellantoni⁵¹, A. Bellavance⁵¹, J.A. Benitez⁶⁶, S.B. Beri²⁷, G. Bernardi¹⁷, R. Bernhard²³, I. Bertram⁴³, M. Besançon¹⁸, R. Beuselinck⁴⁴, V.A. Bezzubov³⁹, P.C. Bhat⁵¹, V. Bhatnagar²⁷, C. Biscarat²⁰, G. Blazey⁵³, F. Blekman⁴⁴, S. Blessing⁵⁰, D. Bloch¹⁹, K. Bloom⁶⁸, A. Boehnlein⁵¹, D. Boline⁶³, T.A. Bolton⁶⁰, G. Borissov⁴³, T. Bose⁷⁸, A. Brandt⁷⁹, R. Brock⁶⁶, G. Brooijmans⁷¹, A. Bross⁵¹, D. Brown⁸², N.J. Buchanan⁵⁰, D. Buchholz⁵⁴, M. Buehler⁸², V. Buescher²², S. Bunichev³⁸, S. Burdin^{43,b}, S. Burke⁴⁶, T.H. Burnett⁸³, C.P. Buszello⁴⁴, J.M. Butler⁶³, P. Calfayan²⁵, S. Calvet¹⁶, J. Cammin⁷², W. Carvalho³, B.C.K. Casey⁵¹, N.M. Cason⁵⁶, H. Castilla-Valdez³³, S. Chakrabarti¹⁸, D. Chakraborty⁵³, K.M. Chan⁵⁶, K. Chan⁶, A. Chandra⁴⁹, F. Charles^{19,†}, E. Cheu⁴⁶, F. Chevallier¹⁴, D.K. Cho⁶³, S. Choi³², B. Choudhary²⁸, L. Christofek⁷⁸, T. Christoudias^{44,†}, S. Cihangir⁵¹, D. Claes⁶⁸, Y. Coadou⁶, M. Cooke⁸¹, W.E. Cooper⁵¹, M. Corcoran⁸¹, F. Couderc¹⁸, M.-C. Cousinou¹⁵, S. Crépe-Renaudin¹⁴, D. Cutts⁷⁸, M. Cwiok³⁰, H. da Motta², A. Das⁴⁶, G. Davies⁴⁴, K. De⁷⁹, S.J. de Jong³⁵, E. De La Cruz-Burelo⁶⁵, C. De Oliveira Martins³, J.D. Degenhardt⁶⁵, F. Déliot¹⁸, M. Demarteau⁵¹, R. Demina⁷², D. Denisov⁵¹, S.P. Denisov³⁹, S. Desai⁵¹, H.T. Diehl⁵¹, M. Diesburg⁵¹, A. Dominguez⁶⁸, H. Dong⁷³, L.V. Dudko³⁸, L. Duflot¹⁶, S.R. Dugad²⁹, D. Duggan⁵⁰, A. Duperrin¹⁵, J. Dyer⁶⁶, A. Dyshkant⁵³, M. Eads⁶⁸, D. Edmunds⁶⁶, J. Ellison⁴⁹, V.D. Elvira⁵¹, Y. Enari⁷⁸, S. Eno⁶², P. Ermolov³⁸, H. Evans⁵⁵, A. Evdokimov⁷⁴, V.N. Evdokimov³⁹, A.V. Ferapontov⁶⁰, T. Ferbel⁷², F. Fiedler²⁴, F. Filthaut³⁵, W. Fisher⁵¹, H.E. Fisk⁵¹, M. Ford⁴⁵, M. Fortner⁵³, H. Fox²³, S. Fu⁵¹, S. Fuess⁵¹, T. Gadfort⁸³, C.F. Galea³⁵, E. Gallas⁵¹, E. Galyaev⁵⁶, C. Garcia⁷², A. Garcia-Bellido⁸³, V. Gavrilov³⁷, P. Gay¹³, W. Geist¹⁹, D. Gelé¹⁹, C.E. Gerber⁵², Y. Gershtein⁵⁰, D. Gillberg⁶, G. Ginther⁷², N. Gollub⁴¹, B. Gómez⁸, A. Goussiou⁵⁶, P.D. Grannis⁷³, H. Greenlee⁵¹, Z.D. Greenwood⁶¹, E.M. Gregores⁴, G. Grenier²⁰, Ph. Gris¹³, J.-F. Grivaz¹⁶, A. Grohsjean²⁵, S. Grünendahl⁵¹, M.W. Grünewald³⁰, J. Guo⁷³, F. Guo⁷³, P. Gutierrez⁷⁶, G. Gutierrez⁵¹, A. Haas⁷¹, N.J. Hadley⁶², P. Haefner²⁵, S. Hagopian⁵⁰, J. Haley⁶⁹, I. Hall⁶⁶, R.E. Hall⁴⁸, L. Han⁷, K. Hanagaki⁵¹, P. Hansson⁴¹, K. Harder⁴⁵, A. Harel⁷², R. Harrington⁶⁴, J.M. Hauptman⁵⁸, R. Hauser⁶⁶, J. Hays⁴⁴, T. Hebbeker²¹, D. Hedin⁵³, J.G. Hegeman³⁴, J.M. Heinmiller⁵², A.P. Heinson⁴⁹, U. Heintz⁶³, C. Hensel⁵⁹, K. Herner⁷³, G. Hesketh⁶⁴, M.D. Hildreth⁵⁶, R. Hirosky⁸², J.D. Hobbs⁷³, B. Hoeneisen¹², H. Hoeth²⁶, M. Hohlfeld²², S.J. Hong³¹, S. Hossain⁷⁶, P. Houben³⁴, Y. Hu⁷³, Z. Hubacek¹⁰, V. Hynek⁹, I. Iashvili⁷⁰, R. Illingworth⁵¹, A.S. Ito⁵¹, S. Jabeen⁶³, M. Jaffré¹⁶, S. Jain⁷⁶, K. Jakobs²³, C. Jarvis⁶², R. Jesik⁴⁴, K. Johns⁴⁶, C. Johnson⁷¹, M. Johnson⁵¹, A. Jonckheere⁵¹, P. Jonsson⁴⁴, A. Juste⁵¹, D. Käfer²¹, E. Kajfasz¹⁵, A.M. Kalinin³⁶, J.R. Kalk⁶⁶, J.M. Kalk⁶¹, S. Kappler²¹, D. Karmanov³⁸, P. Kasper⁵¹, I. Katsanos⁷¹, D. Kau⁵⁰, R. Kaur²⁷, V. Kaushik⁷⁹, R. Kehoe⁸⁰, S. Kermiche¹⁵, N. Khalatyan⁵¹, A. Khanov⁷⁷, A. Kharchilava⁷⁰, Y.M. Kharzheev³⁶, D. Khatidze⁷¹, H. Kim³², T.J. Kim³¹, M.H. Kirby⁵⁴, M. Kirsch²¹, B. Klima⁵¹, J.M. Kohli²⁷, J.-P. Konrath²³, M. Kopal⁷⁶, V.M. Korablev³⁹, A.V. Kozelov³⁹, D. Krop⁵⁵, T. Kuhl²⁴, A. Kumar⁷⁰, S. Kunori⁶², A. Kupco¹¹, T. Kurča²⁰, J. Kvita⁹, F. Lacroix¹³, D. Lam⁵⁶, S. Lammers⁷¹, G. Landsberg⁷⁸, P. Lebrun²⁰, W.M. Lee⁵¹, A. Leflat³⁸, F. Lehner⁴², J. Lellouch¹⁷, J. Leveque⁴⁶, P. Lewis⁴⁴, J. Li⁷⁹, Q.Z. Li⁵¹, L. Li⁴⁹, S.M. Lietti⁵, J.G.R. Lima⁵³, D. Lincoln⁵¹, J. Linnemann⁶⁶, V.V. Lipaev³⁹, R. Lipton⁵¹, Y. Liu^{7,†}, Z. Liu⁶, L. Lobo⁴⁴, A. Lobodenko⁴⁰, M. Lokajicek¹¹, P. Love⁴³, H.J. Lubatti⁸³, A.L. Lyon⁵¹, A.K.A. Maciel², D. Mackin⁸¹, R.J. Madaras⁴⁷, P. Mättig²⁶, C. Magass²¹, A. Magerkurth⁶⁵, P.K. Mal⁵⁶, H.B. Malbouisson³, S. Malik⁶⁸, V.L. Malyshev³⁶, H.S. Mao⁵¹, Y. Maravin⁶⁰, B. Martin¹⁴, R. McCarthy⁷³, A. Melnitchouk⁶⁷, A. Mendes¹⁵, L. Mendoza⁸, P.G. Mercadante⁵, M. Merkin³⁸, K.W. Merritt⁵¹, J. Meyer^{22,d}, A. Meyer²¹, T. Millet²⁰, J. Mitrevski⁷¹, J. Molina³, R.K. Mommsen⁴⁵, N.K. Mondal²⁹, R.W. Moore⁶, T. Moulik⁵⁹, G.S. Muanza²⁰, M. Mulders⁵¹, M. Mulhearn⁷¹, O. Mundal²², L. Mundim³, E. Nagy¹⁵, M. Naimuddin⁵¹, M. Narain⁷⁸, N.A. Naumann³⁵, H.A. Neal⁶⁵, J.P. Negret⁸, P. Neustroev⁴⁰, H. Nilsen²³, H. Nogima³, A. Nomerotski⁵¹, S.F. Novaes⁵, T. Nunnemann²⁵, V. O'Dell⁵¹, D.C. O'Neil⁶, G. Obrant⁴⁰, C. Ochando¹⁶, D. Onoprienko⁶⁰, N. Oshima⁵¹, J. Osta⁵⁶, R. Otec¹⁰, G.J. Otero y Garzón⁵¹, M. Owen⁴⁵, P. Padley⁸¹, M. Pangilinan⁷⁸, N. Parashar⁵⁷,

S.-J. Park⁷², S.K. Park³¹, J. Parsons⁷¹, R. Partridge⁷⁸, N. Parua⁵⁵, A. Patwa⁷⁴, G. Pawloski⁸¹, B. Penning²³, M. Perfilov³⁸, K. Peters⁴⁵, Y. Peters²⁶, P. Pétrouff¹⁶, M. Petteni⁴⁴, R. Piegai¹, J. Piper⁶⁶, M.-A. Pleier²², P.L.M. Podesta-Lerma^{33,c}, V.M. Podstavkov⁵¹, Y. Pogorelov⁵⁶, M.-E. Pol², P. Polozov³⁷, B.G. Pope⁶⁶, A.V. Popov³⁹, C. Potter⁶, W.L. Prado da Silva³, H.B. Prosper⁵⁰, S. Protopopescu⁷⁴, J. Qian⁶⁵, A. Quadt^{22,d}, B. Quinn⁶⁷, A. Rakitine⁴³, M.S. Rangel², K. Ranjan²⁸, P.N. Ratoff⁴³, P. Renkel⁸⁰, S. Reucroft⁶⁴, P. Rich⁴⁵, M. Rijssenbeek⁷³, I. Ripp-Baudot¹⁹, F. Rizatdinova⁷⁷, S. Robinson⁴⁴, R.F. Rodrigues³, M. Rominsky⁷⁶, C. Royon¹⁸, P. Rubinov⁵¹, R. Ruchti⁵⁶, G. Safronov³⁷, G. Sajot¹⁴, A. Sánchez-Hernández³³, M.P. Sanders¹⁷, A. Santoro³, G. Savage⁵¹, L. Sawyer⁶¹, T. Scanlon⁴⁴, D. Schaile²⁵, R.D. Schamberger⁷³, Y. Scheglov⁴⁰, H. Schellman⁵⁴, P. Schieferdecker²⁵, T. Schliephake²⁶, C. Schwanenberger⁴⁵, A. Schwartzman⁶⁹, R. Schwienhorst⁶⁶, J. Sekaric⁵⁰, H. Severini⁷⁶, E. Shabalina⁵², M. Shamim⁶⁰, V. Shary¹⁸, A.A. Shchukin³⁹, R.K. Shivpuri²⁸, V. Siccaldi¹⁹, V. Simak¹⁰, V. Sirotenko⁵¹, P. Skubic⁷⁶, P. Slattery⁷², D. Smirnov⁵⁶, J. Snow⁷⁵, G.R. Snow⁶⁸, S. Snyder⁷⁴, S. Söldner-Rembold⁴⁵, L. Sonnenschein¹⁷, A. Sopczak⁴³, M. Sosebee⁷⁹, K. Soustruznik⁹, M. Souza², B. Spurlock⁷⁹, J. Stark¹⁴, J. Steele⁶¹, V. Stolin³⁷, D.A. Stoyanova³⁹, J. Strandberg⁶⁵, S. Strandberg⁴¹, M.A. Strang⁷⁰, M. Strauss⁷⁶, E. Strauss⁷³, R. Ströhmer²⁵, D. Strom⁵⁴, L. Stutte⁵¹, S. Sumowidagdo⁵⁰, P. Svoisky⁵⁶, A. Sznajder³, M. Talby¹⁵, P. Tamburello⁴⁶, A. Tanasijczuk¹, W. Taylor⁶, J. Temple⁴⁶, B. Tiller²⁵, F. Tissandier¹³, M. Titov¹⁸, V.V. Tokmenin³⁶, T. Toole⁶², I. Torchiani²³, T. Trefzger²⁴, D. Tsybychev⁷³, B. Tuchming¹⁸, C. Tully⁶⁹, P.M. Tuts⁷¹, R. Unalan⁶⁶, S. Uvarov⁴⁰, L. Uvarov⁴⁰, S. Uzunyan⁵³, B. Vachon⁶, P.J. van den Berg³⁴, R. Van Kooten⁵⁵, W.M. van Leeuwen³⁴, N. Varelas⁵², E.W. Varnes⁴⁶, I.A. Vasilyev³⁹, M. Vaupel²⁶, P. Verdier²⁰, L.S. Vertogradov³⁶, M. Verzocchi⁵¹, F. Villeneuve-Segui⁴⁴, P. Vint⁴⁴, P. Vokac¹⁰, E. Von Toerne⁶⁰, M. Voutilainen^{68,e}, R. Wagner⁶⁹, H.D. Wahl⁵⁰, L. Wang⁶², M.H.L.S. Wang⁵¹, J. Warchol⁵⁶, G. Watts⁸³, M. Wayne⁵⁶, M. Weber⁵¹, G. Weber²⁴, A. Wenger^{23,f}, N. Vermes²², M. Wetstein⁶², A. White⁷⁹, D. Wicke²⁶, G.W. Wilson⁵⁹, S.J. Wimpenny⁴⁹, M. Wobisch⁶¹, D.R. Wood⁶⁴, T.R. Wyatt⁴⁵, Y. Xie⁷⁸, S. Yacoob⁵⁴, R. Yamada⁵¹, M. Yan⁶², T. Yasuda⁵¹, Y.A. Yatsunenko³⁶, K. Yip⁷⁴, H.D. Yoo⁷⁸, S.W. Youn⁵⁴, J. Yu⁷⁹, A. Zatserklyaniy⁵³, C. Zeitnitz²⁶, T. Zhao⁸³, B. Zhou⁶⁵, J. Zhu⁷³, M. Zielinski⁷², D. Zieminska⁵⁵, A. Zieminski⁵⁵, L. Zivkovic⁷¹, V. Zutshi⁵³, and E.G. Zverev³⁸

(The DØ Collaboration)

¹Universidad de Buenos Aires, Buenos Aires, Argentina

²LAFEX, Centro Brasileiro de Pesquisas Físicas, Rio de Janeiro, Brazil

³Universidade do Estado do Rio de Janeiro, Rio de Janeiro, Brazil

⁴Universidade Federal do ABC, Santo André, Brazil

⁵Instituto de Física Teórica, Universidade Estadual Paulista, São Paulo, Brazil

⁶University of Alberta, Edmonton, Alberta, Canada,

Simon Fraser University, Burnaby, British Columbia,

Canada, York University, Toronto, Ontario, Canada,

and McGill University, Montreal, Quebec, Canada

⁷University of Science and Technology of China, Hefei, People's Republic of China

⁸Universidad de los Andes, Bogotá, Colombia

⁹Center for Particle Physics, Charles University, Prague, Czech Republic

¹⁰Czech Technical University, Prague, Czech Republic

¹¹Center for Particle Physics, Institute of Physics, Academy of Sciences of the Czech Republic, Prague, Czech Republic

¹²Universidad San Francisco de Quito, Quito, Ecuador

¹³Laboratoire de Physique Corpusculaire, IN2P3-CNRS, Université Blaise Pascal, Clermont-Ferrand, France

¹⁴Laboratoire de Physique Subatomique et de Cosmologie, IN2P3-CNRS, Université de Grenoble 1, Grenoble, France

¹⁵CPPM, IN2P3-CNRS, Université de la Méditerranée, Marseille, France

¹⁶Laboratoire de l'Accélérateur Linéaire, IN2P3-CNRS et Université Paris-Sud, Orsay, France

¹⁷LPNHE, IN2P3-CNRS, Universités Paris VI and VII, Paris, France

¹⁸DAPNIA/Service de Physique des Particules, CEA, Saclay, France

¹⁹IPHC, Université Louis Pasteur et Université de Haute Alsace, CNRS, IN2P3, Strasbourg, France

²⁰IPNL, Université Lyon 1, CNRS/IN2P3, Villeurbanne, France and Université de Lyon, Lyon, France

²¹III. Physikalisches Institut A, RWTH Aachen, Aachen, Germany

²²Physikalisches Institut, Universität Bonn, Bonn, Germany

²³Physikalisches Institut, Universität Freiburg, Freiburg, Germany

²⁴Institut für Physik, Universität Mainz, Mainz, Germany

²⁵Ludwig-Maximilians-Universität München, München, Germany

²⁶Fachbereich Physik, University of Wuppertal, Wuppertal, Germany

- ²⁷ Panjab University, Chandigarh, India
²⁸ Delhi University, Delhi, India
²⁹ Tata Institute of Fundamental Research, Mumbai, India
³⁰ University College Dublin, Dublin, Ireland
³¹ Korea Detector Laboratory, Korea University, Seoul, Korea
³² SungKyunKwan University, Suwon, Korea
³³ CINVESTAV, Mexico City, Mexico
³⁴ FOM-Institute NIKHEF and University of Amsterdam/NIKHEF, Amsterdam, The Netherlands
³⁵ Radboud University Nijmegen/NIKHEF, Nijmegen, The Netherlands
³⁶ Joint Institute for Nuclear Research, Dubna, Russia
³⁷ Institute for Theoretical and Experimental Physics, Moscow, Russia
³⁸ Moscow State University, Moscow, Russia
³⁹ Institute for High Energy Physics, Protvino, Russia
⁴⁰ Petersburg Nuclear Physics Institute, St. Petersburg, Russia
⁴¹ Lund University, Lund, Sweden, Royal Institute of Technology and Stockholm University, Stockholm, Sweden, and Uppsala University, Uppsala, Sweden
⁴² Physik Institut der Universität Zürich, Zürich, Switzerland
⁴³ Lancaster University, Lancaster, United Kingdom
⁴⁴ Imperial College, London, United Kingdom
⁴⁵ University of Manchester, Manchester, United Kingdom
⁴⁶ University of Arizona, Tucson, Arizona 85721, USA
⁴⁷ Lawrence Berkeley National Laboratory and University of California, Berkeley, California 94720, USA
⁴⁸ California State University, Fresno, California 93740, USA
⁴⁹ University of California, Riverside, California 92521, USA
⁵⁰ Florida State University, Tallahassee, Florida 32306, USA
⁵¹ Fermi National Accelerator Laboratory, Batavia, Illinois 60510, USA
⁵² University of Illinois at Chicago, Chicago, Illinois 60607, USA
⁵³ Northern Illinois University, DeKalb, Illinois 60115, USA
⁵⁴ Northwestern University, Evanston, Illinois 60208, USA
⁵⁵ Indiana University, Bloomington, Indiana 47405, USA
⁵⁶ University of Notre Dame, Notre Dame, Indiana 46556, USA
⁵⁷ Purdue University Calumet, Hammond, Indiana 46323, USA
⁵⁸ Iowa State University, Ames, Iowa 50011, USA
⁵⁹ University of Kansas, Lawrence, Kansas 66045, USA
⁶⁰ Kansas State University, Manhattan, Kansas 66506, USA
⁶¹ Louisiana Tech University, Ruston, Louisiana 71272, USA
⁶² University of Maryland, College Park, Maryland 20742, USA
⁶³ Boston University, Boston, Massachusetts 02215, USA
⁶⁴ Northeastern University, Boston, Massachusetts 02115, USA
⁶⁵ University of Michigan, Ann Arbor, Michigan 48109, USA
⁶⁶ Michigan State University, East Lansing, Michigan 48824, USA
⁶⁷ University of Mississippi, University, Mississippi 38677, USA
⁶⁸ University of Nebraska, Lincoln, Nebraska 68588, USA
⁶⁹ Princeton University, Princeton, New Jersey 08544, USA
⁷⁰ State University of New York, Buffalo, New York 14260, USA
⁷¹ Columbia University, New York, New York 10027, USA
⁷² University of Rochester, Rochester, New York 14627, USA
⁷³ State University of New York, Stony Brook, New York 11794, USA
⁷⁴ Brookhaven National Laboratory, Upton, New York 11973, USA
⁷⁵ Langston University, Langston, Oklahoma 73050, USA
⁷⁶ University of Oklahoma, Norman, Oklahoma 73019, USA
⁷⁷ Oklahoma State University, Stillwater, Oklahoma 74078, USA
⁷⁸ Brown University, Providence, Rhode Island 02912, USA
⁷⁹ University of Texas, Arlington, Texas 76019, USA
⁸⁰ Southern Methodist University, Dallas, Texas 75275, USA
⁸¹ Rice University, Houston, Texas 77005, USA
⁸² University of Virginia, Charlottesville, Virginia 22901, USA and
⁸³ University of Washington, Seattle, Washington 98195, USA

(Dated: October 21,2007)

We report results of a search for supersymmetry (SUSY) with gauge-mediated symmetry breaking in di-photon events collected by the D0 experiment at the Fermilab Tevatron Collider in 2002–2006. In 1.1 fb^{-1} of data, we find no significant excess beyond the background expected from the standard model and set the most stringent lower limits to date for a standard benchmark model on the lightest

neutralino and chargino masses of 125 GeV and 229 GeV, respectively, at 95% confidence.

PACS numbers: 14.80.Ly, 12.60.Jv, 13.85.Rm

Low-scale SUSY is one of the most promising solutions to the hierarchy problem associated with the intrinsic disparity between the electroweak and Planck scales. It postulates that for each known particle there exists a superpartner, thereby stabilizing the radiative corrections to the Higgs boson mass. Bosons have fermion superpartners, and vice versa. None of the superpartners have yet been observed, and superpartner masses must therefore be much larger than those of their partners, *i.e.*, SUSY is a broken symmetry. Experimental signatures of supersymmetry are determined through the manner and scale of SUSY breaking. In models with gauge-mediated supersymmetry breaking (GMSB) [1, 2], it is achieved through the introduction of new chiral supermultiplets, called messengers that couple to the ultimate source of supersymmetry breaking and to the SUSY particles. At colliders, assuming R -parity conservation [3], superpartners are produced in pairs ($\tilde{\chi}_1^+ \tilde{\chi}_1^-$ and $\tilde{\chi}_1^\pm \tilde{\chi}_2^0$ production dominates in most cases) and decay to the standard model particles and next-to-lightest SUSY particle (NLSP), which can be either a neutralino or a slepton. In the former case, which is considered in this note, the NLSP decays into a photon and a gravitino (the lightest superpartner in GMSB SUSY models, with mass less than ≈ 1 keV). The gravitino is stable, and escapes detection, creating an apparent imbalance in transverse momentum (\cancel{E}_T) in the event. GMSB SUSY final states are therefore characterized by two energetic photons and large missing transverse momentum. The differences in event kinematics between particular GMSB SUSY models result in slightly different experimental sensitivities [1], and to obtain a quantitative measure of limits on SUSY we consider a model referred to as ‘‘Snowmass Slope SPS 8’’ [4]. This model has only a single dimensioned parameter: an energy scale Λ that determines the effective scale of SUSY breaking. The minimal GMSB parameters correspond to a messenger mass $M_m = 2\Lambda$, the number of messengers $N_5 = 1$, the ratio of the vacuum expectation values of the two Higgs fields $\tan\beta = 15$, and the sign of the Higgsino mass term $\mu > 0$. The neutralino lifetime is not defined within the model. For this analysis, it is assumed to be sufficiently short to yield decays with prompt photons.

Searches for GMSB SUSY were carried out by collaborations at the CERN LEP collider [5] and at the Fermilab Tevatron collider in both Run I [6] and early in Run II [7, 8]. The initial limits from CDF and D0 for Run II, based on the SPS 8 model, were combined [9] to yield $\Lambda > 84.6$ TeV corresponding to the limit on the chargino mass of 209 GeV, at 95% confidence. Complementary searches for GMSB SUSY with R -parity violation were performed by the H1 experiment at HERA [10].

This analysis is an update of that described in Ref. [7], with about a factor of three more data and improved photon identification based on: (i) an electromagnetic (EM) cluster ‘‘pointing’’ algorithm that predicts the origin of a photon with a resolution of about 2 cm along the beam axis, thereby eliminating the largest instrumental background associated with misreconstruction of the primary interaction vertex, and (ii) an improved track veto requirement that suppresses sources of background with electrons in the final state. We also use an improved likelihood fitter [11] to set limits on the scale parameter Λ .

The data in this analysis were recorded using single EM triggers with the D0 detector [12], the main components of which are an inner tracker, liquid-argon/uranium calorimeters, and a muon spectrometer. The inner tracker consists of silicon microstrip and central scintillating-fiber trackers located in a 2 T superconducting solenoidal magnet, providing measurements up to pseudorapidities¹ of $|\eta| \approx 3.0$ and $|\eta| \approx 1.8$, respectively. The calorimeters are finely segmented and consist of a central section (CC) covering $|\eta| < 1.2$ and two end-cap calorimeters extending coverage to $|\eta| \approx 4$, all housed in separate cryostats [13]. The electromagnetic section of the calorimeter has four longitudinal layers and transverse segmentation of 0.1×0.1 in $\eta - \phi$ space (where ϕ is the azimuthal angle), except in the third layer, where it is 0.05×0.05 . The central preshower (CPS) system is placed between the solenoid and the calorimeter cryostat and covers $|\eta| \lesssim 1.2$. The CPS provides precise measurement of positions of EM showers. The axes of EM showers are reconstructed by fitting straight lines to shower positions measured in the four longitudinal calorimeter layers and the CPS (EM ‘‘pointing’’). The data for this study were collected between 2002 and summer 2006, using inclusive single EM triggers that are almost 100% efficient to select signal data. The integrated luminosity [14] of the sample is 1100 ± 70 pb⁻¹.

Photons and electrons are identified based on reconstructed EM clusters using calorimetric information and further classified into electron and photon candidates, based on tracking information. The EM clusters are selected from calorimeter clusters using the simple cone method (of radius $\mathcal{R} = \sqrt{(\Delta\eta)^2 + (\Delta\phi)^2} = 0.4$) by requiring that (i) at least 90% of the energy is deposited in the EM section of the calorimeter, (ii) the calorimeter isolation variable $I = [E_{\text{tot}}(0.4) - E_{EM}(0.2)]/E_{EM}(0.2)$ is less than 0.07, where $E_{\text{tot}}(0.4)$ is the total shower en-

¹ Pseudorapidity is defined as $-\log(\tan(\frac{\theta}{2}))$, where θ is the angle between the particle and the proton beam direction.

ergy in a cone of radius $\mathcal{R} = 0.4$, and $E_{EM}(0.2)$ is the EM energy in a cone of radius $\mathcal{R} = 0.2$, (iii) the transverse, energy-weighted, width of the EM cluster in the third EM calorimeter layer is smaller than 0.04 rad, and (iv) the scalar sum of the transverse momenta (p_T) of all tracks originating from the primary vertex in an annulus of $0.05 < \mathcal{R} < 0.4$ around the cluster is less than 2 GeV. The EM cluster is further defined as an electron candidate if it is spatially matched to activity in the tracker, and as a photon candidate otherwise. The tracker activity can be either a reconstructed track or a density of hits in the silicon microstrip and central fiber trackers consistent with a track, i.e., an electron. The latter requirement allows for increasing electron track-matching efficiency, ϵ_{trk} , measured in $Z \rightarrow ee$ data, from $(93.0 \pm 0.1)\%$ to $(98.6 \pm 0.1)\%$ by identifying electrons with lost tracks due to hard bremsstrahlung and/or inefficiency of the inner trackers. This reduces electron backgrounds to photons by a factor of five, while keeping the efficiency of anti-track activity requirement high. We measure that $(91 \pm 3)\%$ of photon candidates in $Z \rightarrow ee\gamma$ data satisfy the anti-track activity requirement.

Jets are reconstructed using the iterative, midpoint cone algorithm [15] with a cone size of $\mathcal{R} = 0.5$. The missing transverse energy is determined from the energy deposited in the calorimeter for $|\eta| < 4$ and is corrected for the EM and jet energy scales.

We select $\gamma\gamma$ candidates by requiring events to have two photon candidates, each with transverse energy $E_T > 25$ GeV identified in the CC with $|\eta| < 1.1$. We require that at least one of the photon candidates be matched to a CPS cluster, and that the primary vertex be consistent with that of the photon candidate (obtained from the EM pointing). The accuracy of the determination of the photon vertex is measured using photons from final state radiation in $Z \rightarrow ee\gamma$ data sample and found to be 2.3 ± 0.3 cm. The requirement of consistency between the photon and primary vertices ensures correct calculation of the transverse energies and tracking isolation requirements. The accuracy of primary vertex association is studied in GMSB SUSY Monte Carlo simulated events, where the primary vertex is identified correctly in $(98.5 \pm 0.1)\%$ of the events while the photon vertex matches the primary vertex in $(95.8 \pm 0.1)\%$.

To reduce potential bias in the measurement of \cancel{E}_T from mismeasurement of jet transverse momentum, we also require that the jet with the highest E_T (if jets are present in the event) be separated from the \cancel{E}_T in azimuth by no more than 2.5 radians. This selection yields 2341 events (the $\gamma\gamma$ sample).

All instrumental backgrounds arise from standard model processes, with either genuine \cancel{E}_T ($W\gamma$, W +jet, and $t\bar{t}$ production) or without inherent \cancel{E}_T (direct photon, multi-jet, and $Z \rightarrow ee$ production). All these backgrounds are measured using data.

The former source always has an electron in the final

state which is misidentified as a photon. The contribution of this background to the \cancel{E}_T distribution in data can be estimated using an $e\gamma$ sample (selected by requiring an electron and a photon candidate and using the same kinematical requirements as for the $\gamma\gamma$ sample) scaled by the probability of an electron-photon misidentification which is measured using $Z \rightarrow ee$ data. First, the \cancel{E}_T distribution in the $e\gamma$ sample must be corrected for the contribution from events with no real \cancel{E}_T . The contribution from Drell-Yan events is taken into account by obtaining the \cancel{E}_T distribution for the ee sample (selected by requiring two electron candidates and applying the same kinematical requirements as for the $\gamma\gamma$ sample) which is dominated by Drell-Yan events. The Drell-Yan \cancel{E}_T distribution is further normalized to the number of Z boson events in the $e\gamma$ sample (the latter is determined by fitting the $e\gamma$ invariant mass spectrum to the Z boson mass peak).

The contribution from the multi-jet processes is estimated from a data sample (referred to as the QCD sample) selected by requiring two EM clusters that (a) satisfy all the kinematic selection used to select $\gamma\gamma$ sample and (b) satisfy all the photon identification criteria but fail the shower shape requirement. The \cancel{E}_T distribution in the QCD sample is normalized to the number of the events in the $e\gamma$ sample with $\cancel{E}_T < 12$ GeV after subtraction of the Drell-Yan contribution as determined above. The expected number of $W\gamma$, W +jet, and $t\bar{t}$ events with $\cancel{E}_T < 12$ GeV is negligible.

After the Drell-Yan and multi-jet contributions to the $e\gamma$ sample are subtracted, the resulting \cancel{E}_T distribution is scaled by $(1 - \epsilon_{\text{trk}})/\epsilon_{\text{trk}}$, where ϵ_{trk} is the efficiency of the track-matching requirement to obtain the estimate of \cancel{E}_T distribution for the background with genuine \cancel{E}_T .

The background from events with no inherent \cancel{E}_T is divided into multi-jet events with two real isolated photons and events where one or both photons are misidentified jets. Since the \cancel{E}_T resolution for both sources is dominated by the photon energy resolution, the \cancel{E}_T distributions for the two sources are very similar. However, misidentified jets have a different energy response compared with that of real photons which leads to a slight difference in the shapes of the \cancel{E}_T distributions. For the real di-photon events, the \cancel{E}_T is assumed to have the same shape as that of the Drell-Yan events. For misidentified jets, the shape of the \cancel{E}_T distribution is taken from the QCD sample. Relative normalization of the two sources is obtained using a fit to the \cancel{E}_T distribution in the $\gamma\gamma$ sample. We check that the fit is not sensitive to possible signal contribution, and cross-check with a method that estimates the $\gamma\gamma$ sample purity using the measured shower shape in the CPS. The relative fraction of di-photons is $(60 \pm 20)\%$ and this uncertainty is propagated as a systematic uncertainty for the limit setting. Absolute normalization of the \cancel{E}_T distributions from both sources is determined so

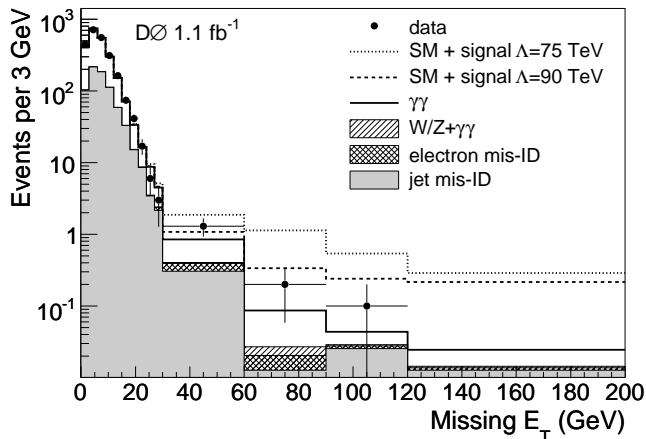


FIG. 1: The \cancel{E}_T distribution in $\gamma\gamma$ data with $W/Z + \gamma\gamma$ background (hatched histogram), instrumental background with no genuine \cancel{E}_T : $\gamma\gamma$ (solid black line) and multi-jet (filled histogram), and background from processes with genuine \cancel{E}_T and a misidentified electron (cross-hatched histogram). The expected \cancel{E}_T distributions if GMSB SUSY events were present are shown as dotted and dashed lines.

that the number of events with $\cancel{E}_T < 12$ GeV matches that in the $\gamma\gamma$ sample.

The largest physics backgrounds are from $Z\gamma\gamma \rightarrow \nu\nu\gamma\gamma$ and $W\gamma\gamma \rightarrow \ell\gamma\gamma\nu$ processes. Contributions from these backgrounds are estimated as 0.15 ± 0.06 and 0.10 ± 0.04 events, respectively, using COMPHEP [16] Monte Carlo simulation, cross-checked with MADGRAPH [17]. The contribution of these backgrounds to the \cancel{E}_T distribution is taken from Monte Carlo simulation, with number of events normalized to the integrated luminosity of the data sample.

The \cancel{E}_T distribution for the $\gamma\gamma$ sample, with contributions from physics background ($W/Z + \gamma\gamma$), and instrumental background with genuine \cancel{E}_T (processes with misidentified electrons) and no inherent \cancel{E}_T ($\gamma\gamma$ and multi-jet) is given in Fig 1. We also illustrate the \cancel{E}_T distribution expected from GMSB SUSY for two values of Λ . The number of observed events, as well as expected background and signal from GMSB SUSY for $\cancel{E}_T > 30$ GeV and > 60 GeV are given in Table I.

The expected GMSB signal efficiency is estimated from Monte Carlo simulation generated for several points on the Snowmass Slope (see Table II), covering the neutralino mass range from 170 GeV to 280 GeV. Although $\tilde{\chi}_1^+ \tilde{\chi}_1^-$ and $\tilde{\chi}_1^\pm \tilde{\chi}_2^0$ processes dominate, we consider all GMSB SUSY production channels. We used ISAJET 7.58 [18] to determine SUSY interaction eigenstate masses and couplings. PYTHIA 6.319 [19] is used to generate the events after determining the sparticle masses, branching fractions and leading order (LO) production cross sections using CTEQ6L1 parton distributions [20]. The generated events are processed through

a full GEANT-based [21] detector simulation and the same reconstruction code as used for data. The LO signal cross sections are scaled to match the next-to-leading order (NLO) prediction using k -factor values (see Table II), extracted from Ref. [22].

The systematic error on the expected number of signal events comes from the uncertainties in photon identification efficiency (10%), statistics in MC samples (5%), track veto requirement (3%), and trigger efficiency (4%). These were obtained using $Z \rightarrow e^+e^-$ and $Z \rightarrow e^+e^-\gamma$ decays in data and in MC simulation. Variation of parton distribution functions and uncertainty in the total integrated luminosity result in additional 4% and 6.1% errors in signal yield respectively. The total uncertainty on the background is dominated by statistics.

As the observed number of events for all values of \cancel{E}_T is in good agreement with the standard model prediction, we conclude that there is no evidence for GMSB SUSY in the data. We set limits on the production cross section by utilizing a likelihood fitter [11] that incorporates a log-likelihood ratio (LLR) test statistic method. This method utilizes binned \cancel{E}_T distributions rather than a single-bin (fully-integrated) value, and therefore accounts for the shapes of the distributions, leading to greater sensitivity. The value of the confidence level for the signal CL_s is defined as $CL_s = CL_{s+b}/CL_b$, where CL_{s+b} and CL_b are the confidence levels for the signal plus background hypothesis and the background-only (null) hypothesis, respectively. These confidence levels are evaluated by integrating corresponding LLR distributions populated by simulating outcomes via Poisson statistics. Systematic uncertainties are treated as uncertainties on the expected numbers of signal and background events, not the outcomes of the limit calculations. The degrading effects of systematic uncertainties are reduced by introducing a maximum likelihood fit to the missing transverse energy distribution. A separate fit is performed for both the background-only and signal-plus-background hypotheses for each data or pseudo-data distribution.

The limits are shown in Fig. 2 together with expected signal cross sections. The observed limits are statistically compatible with the expected limits. The observed upper limit on the signal cross section is below the prediction of the Snowmass Slope model for $\Lambda < 91.5$ TeV, or in terms of gaugino masses, $m_{\tilde{\chi}_1^0} < 125$ GeV and $m_{\tilde{\chi}_1^+} < 229$ GeV. These represent the most stringent limits on this particular GMSB SUSY model to date.

We thank the staffs at Fermilab and collaborating institutions, and acknowledge support from the DOE and NSF (USA); CEA and CNRS/IN2P3 (France); FASI, Rosatom and RFBR (Russia); CAPES, CNPq, FAPERJ, FAPESP and FUNDUNESP (Brazil); DAE and DST (India); Colciencias (Colombia); CONACyT (Mexico); KRF and KOSEF (Korea); CONICET and UBACyT (Argentina); FOM (The Netherlands); Science and Tech-

	Genuine \cancel{E}_T	Background events		Total	Expected signal events		Observed events
		No \cancel{E}_T	Physics		$\Lambda = 75$ TeV	$\Lambda = 90$ TeV	
$\cancel{E}_T > 30$ GeV	0.97 ± 0.12	9.62 ± 1.12	0.19 ± 0.07	10.8 ± 1.1	28.3 ± 4.2	8.7 ± 1.3	16
$\cancel{E}_T > 60$ GeV	0.11 ± 0.04	1.44 ± 0.43	0.08 ± 0.04	1.6 ± 0.4	18.1 ± 2.7	6.4 ± 1.0	3

TABLE I: Numbers of background events from $W\gamma$, $W + \text{jet}$, and $t\bar{t}$ (Genuine \cancel{E}_T), no inherent \cancel{E}_T (No \cancel{E}_T), $Z\gamma\gamma \rightarrow \nu\nu\gamma\gamma$ and $W\gamma\gamma \rightarrow \ell\gamma\gamma\nu$ (Physics) processes; the total number of expected background events; numbers of expected GMSB SUSY signal events for two values of Λ ; and the observed numbers of events for $\cancel{E}_T > 30$ GeV and 60 GeV. Errors are statistical and systematic combined.

Λ , TeV	$m_{\tilde{\chi}_1^0}$, GeV	$m_{\tilde{\chi}_1^\pm}$, GeV	σ^{LO} , fb	k -factor	Efficiency
70	93.7	168.2	215	1.21	0.17 ± 0.03
75	101.0	182.3	148	1.20	0.18 ± 0.03
80	108.5	198.1	97.5	1.19	0.18 ± 0.03
85	115.8	212.0	65.4	1.18	0.19 ± 0.03
90	123.0	225.8	41.8	1.17	0.19 ± 0.03
95	130.2	239.7	29.5	1.16	0.20 ± 0.03
100	137.4	253.4	20.6	1.15	0.20 ± 0.03
105	144.5	267.0	14.4	1.14	0.18 ± 0.03
110	151.7	280.7	10.3	1.13	0.19 ± 0.03

TABLE II: Points on the GMSB Snowmass Slope model: neutralino and chargino masses, cross sections predicted by PYTHIA, k -factors, and reconstruction efficiencies with total uncertainty.

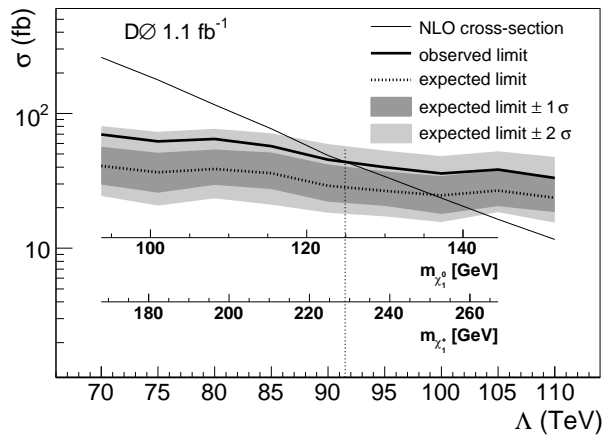


FIG. 2: Predicted cross section for the Snowmass Slope model versus Λ . The observed and expected 95% C.L. limits are shown in solid and dash-dotted lines, respectively.

nology Facilities Council (United Kingdom); MSMT and GACR (Czech Republic); CRC Program, CFI, NSERC and WestGrid Project (Canada); BMBF and DFG (Germany); SFI (Ireland); The Swedish Research Council (Sweden); CAS and CNSF (China); Alexander von Humboldt Foundation; and the Marie Curie Program.

- [a] Visitor from Augustana College, Sioux Falls, SD, USA.
- [b] Visitor from The University of Liverpool, Liverpool, UK.
- [c] Visitor from ICN-UNAM, Mexico City, Mexico.
- [d] Visitor from II. Physikalisches Institut, Georg-August-University Göttingen, Germany.
- [e] Visitor from Helsinki Institute of Physics, Helsinki, Finland.
- [f] Visitor from Universität Zürich, Zürich, Switzerland.
- [†] Fermilab International Fellow.
- [‡] Deceased.

- [1] P. Fayet, Phys. Lett. B **70**, 461 (1977); *ibid.* **86**, 272 (1979); *ibid.* **175**, 471 (1986).
- [2] M. Dine, A. E. Nelson, Y. Nir, and Y. Shirman, Phys. Rev. D **53**, 2658 (1996); H. Baer, M. Brhlik, C. H. Chen, and X. Tata, Phys. Rev. D **55**, 4463 (1997); H. Baer, P. G. Mercadante, X. Tata, and Y. L. Wang, Phys. Rev. D **60**, 055001 (1999); S. Dimopoulos, S. Thomas, and J. D. Wells, Nucl. Phys. B **488**, 39 (1997); J. R. Ellis, J. L. Lopez, and D. V. Nanopoulos, Phys. Lett. B **394**, 354 (1997); see also a review by G. F. Giudice and R. Rattazzi, “Gauge-Mediated Supersymmetry Breaking” in G. L. Kane: *Perspectives on Supersymmetry*, World Scientific, Singapore (1998), p. 355-377, and references therein.
- [3] G.R. Farrar and P. Fayet, Phys. Lett. B **79**, 442 (1978).
- [4] S.P. Martin, S. Moretti, J.M. Qian, and G.W. Wilson, “Direct Investigation of Supersymmetry: Subgroup summary report,” in *Proceedings of the APS/DPF/DPB Summer Study on the Future of Particle Physics (Snowmass 2001)*, edited by N. Graf, eConf **C010630**, p. 346 (2001); B.C. Allanach *et al.*, Eur. Phys. J. C **25**, 113 (2002).
- [5] LEP SUSY Working Group, ALEPH, DELPHI, L3, and OPAL Collaborations, LEPSUSYWG/04-09.1 (<http://lepsusy.web.cern.ch>).
- [6] B. Abbott *et al.*, Phys. Rev. Lett. **80**, 442 (1998); F. Abe *et al.*, Phys. Rev. D **59**, 092002 (1999).
- [7] V. Abazov *et al.*, Phys. Rev. Lett. **94**, 041801 (2005).
- [8] D. Acosta *et al.*, Phys. Rev. D **71**, 031104(R) (2005).
- [9] V. Buescher *et al.*, hep-ex/0504004.
- [10] A. Aktas *et al.*, Phys. Lett. B **616**, 31 (2005).
- [11] W. Fisher, FERMILAB-TM-2386-E (2007); T. Junk, Nucl. Instrum. Methods A **434**, 435 (1999); A. Read, “Modified Frequentist Analysis of Search Results (The CLs Method),” CERN 2000-005 (2000).
- [12] V.M. Abazov *et al.*, Nucl. Instrum. Methods A **565**, 463 (2006).
- [13] S. Abachi, *et al.*, Nucl. Instrum. Methods A **338**, 185

- (1994).
- [14] T. Andeen *et al.*, FERMILAB-TM-2365 (2006).
 - [15] G.C. Blazey *et al.*, in *Proceedings of the Workshop: QCD and Weak Boson Physics in Run II*, edited by U. Baur, R.K. Ellis, and D. Zeppenfeld, FERMILAB-PUB-00/297 (2000).
 - [16] A. Pukhov *et al.*, hep-ph/9908288.
 - [17] F. Maltoni and T. Stelzer, JHEP **0302**, 027 (2003).
 - [18] F.E. Paige, S.D. Protopopescu, H. Baer, and X. Tata, hep-ph/0312045.
 - [19] T. Sjöstrand *et al.*, Comput. Phys. Commun. **135**, 238 (2001).
 - [20] J. Pumplin *et al.*, JHEP **0207**, 012 (2002).
 - [21] R. Brun, F. Carminati, CERN program library long writeup, W5013 (1993).
 - [22] W. Beenakker *et al.*, Phys. Rev. Lett. **83**, 3780 (1999).